Structural Investigation of Supercooled Water Confined in Antifreeze Proteins: Models' Performance Evaluation between Coarse Grained and Atomistic Simulation Models

Nghiep H.V.[1], Hung P.N.[2], and Ly L.[1,2,*]

[1] School of Biotechnology, International University – Vietnam National University, HCMC, Vietnam
[2] Institute for Computational Science and Technology at Ho Chi Minh City, Vietnam
ly.le@hcmiu.edu.vn

Abstract. Antifreeze proteins (AFPs) play an important role as inhibitors of ice crystal growth in the body fluid of living organisms. Nonetheless, the exact mechanism of ice growth inhibition is still poorly understood to experimentally analyze the molecular-scale which strongly requires computer simulation for AFPs' binding site to certain planes of ice crystal. In this research, Coarse-Grained simulation using MARTINI force field was utilized to evaluate stability of helix/β-helix restraints of *M. americanus, L. perenne, M. primoryensis* and *C. Fumiferana* were collected on the Protein Data Bank using high resolution of X-ray diffraction because the β-helix/helix in AFPs' structure play an important role to face ice-binding residues with ice cluster, as receptor and ligand interactions. In results, the root mean square deviations have shown high identity of RMSF between AA-MD and CG-MD simulation in 1HG7 and 3P4G, exceptionally, 1N4I and 3ULT that can be further studied in detail using all-atoms molecular dynamics simulation (AA-MD).

Keywords: Antifreeze protein, Coarse-Grained simulation, helix/beta-helix, MARTINI force field, AA-MD.

1 Introduction

Once the temperature below sub-zero temperatures, ice crystals quickly grow then burst cells. This danger, ice formation, is a big problem for organisms in cold climates however a wide variety of organisms: plants (1,2), fish (3, 4, 5), insects (6, 7, 8) and bacteria (9) avoid damages of growth of ice crystals by producing antifreeze proteins (AFPs) or antifreeze glycoproteins (AFGPs) (10) to protect themselves as under zero temperatures. Fish can be lived at subzero temperature in the presence of specialized antifreeze protein substances in their blood, rather than the presence of salts or

* Corresponding author.

A. Petrosino, L. Maddalena, P. Pala (Eds.): ICIAP 2013 Workshops, LNCS 8158, pp. 344–355, 2013.

additional substances (3, 10, 11). Studies revealed that these antifreeze proteins were isolated substance, which get specific function to protect the fish cold damages.

Up to date, the exact mechanism of AFPs are not jet fully understood but which have open many regards to freeze tolerance, they can survive with the formation of extracellular ice in their bodies, and freeze avoidance in organisms, food processing, pharmaceutical, cryopreservation and ice slurries (12, 13,14, 15). In food industries, the proteins can be significantly used additive compound to improve quality of product, such as making a better texture of ice cream and keeping longer shelf life of fruits and vegetables in supermarkets. Beside, antifreeze proteins can be introduced into yeast, fish, fruits and vegetables to give new beneficial properties to these organisms by genetic modification in cold climate areas. (16, 17).

Although antifreeze proteins function as inhibitors of ice formation at a certain point, they do not stop the growth of ice crystals. Size and shapes of ice crystals are controlled under different types of AFPs (18), known as ice-structuring proteins. According to a difference between melting point and freezing point, the activity of antifreeze proteins can be evaluated as thermal hysteresis (TH) which is currently focusing on complementary between binding regions of an AFP surface and specific ice cluster planes lead to high affinity protein binding to the ice surface, as receptor-ligand interactions (19). The size of the ice surface also affects directly to thermal hysteresis. On bigger ice crystals, the AFP cannot work as well as smaller ice crystals by inhibition of ice growth because of breaking the binding surface of AFP. Besides, the concentration and the type of AFP also effect to thermal hysteresis. The moderate AFP and the hyperactive AFP are two main types used to classify their activity in which the moderate is between 1 and 1.5^0C in fish AFP's and 0.1-0.5^0C in plant AFP's. Further, hyperactive AFP is at almost 5^0C in insect AFPs that base on the residues make up ice binding regions observing the difference in helical AFPs with different numbers of repeats to give more efficiency on the thermal hysteresis using nanoliter osmometer and a microscope in experiment (20).

Many theoretical studies have been proposed for understanding the unclear mechanisms of AFPs, which basically focus on hydrogen bonds to the surface of the ice crystals through a wide variety of folding motifs and are classified into five types based on their structure (Fig. 2). The independently AFP's active isoforms seem to be an important role in the forming hydrogen bonds between Threonine (Thr) residues array on one face of the protein and possible bonding places by their alignment on ice surface, to optimize their efficiency (10). The effect of differing numbers of coils has also been confined in the β-helical insect AFPs (20, 21) in *in vitro* determination by NMR and X-ray crystallography. However, in the study of flounder AFP, has shown no difference of AFP activity in comparison between blocked hydrogen bonds and non-blocked hydrogen bonds (23). After, computer simulation provided more experimental evidences to prove hydrogen bonds do not play a key role in AFP's inhibition of ice growth. (15). Following that way, the mechanism based on biomolecular structure, kinetics and thermodynamics of antifreeze proteins have been invested in dynamics behavior simulation in which all of computational calculations were done by all atoms molecular dynamics simulation (AA-MD) method (18). Molecular dynamics (MD) have become a major routine research tool. In the restricted time and

equipment of my thesis, the coarse grained multi-point model was applied instead AA-MD that decreased computational complexity of MD simulation. Specially, feasible time with CG simulation occurring on microsecond or even millisecond timescale is at least four to six orders of magnitude smaller than AA-MD simulation which contains hundred thousands of atoms in a system for observing rearrangement upon ligand binding and folding, occur on microsecond or even the milliseconds timescale to β-helix AFPs stability, which can afford with desktop computers or limited cores in the high performance computer system.

In this study, CG simulation was employed as a new method of the ocean pout (*Macrozoarces americanus*), called globular type III AFP and three AFPs include perennial ryegrass (*Lolium perenne*), marine bacteria *(Marinomonas primoryensis*) and spruce budworm (*Choristoneura fumiferana*), have not classified type yet which have a same β-helix motif of insect AFP for molecular simulation to evaluate stability of β-helix/helix structures which showed activity at the beginning will be proportional to length or added repeats but decreasing activity come from lengthening the protein beyond nine repeats in type III AFP of ocean fish (24). Therefore, the stability evaluation of AFPs structure is very important in β-helix/helix motif presumably due to amino acid residues and ALA/Thr repeats accumulating steric mismatch with the ice cluster faces for further AA-MD simulation to understand AFPs mechanism in details that hypothesis for increasing thermal hysteresis by direct interaction between binding region and ice/water for a long time up to millisecond by using MD simulations.

2 Materials and Methods

2.1 Coarse Grained Simulation

In a wide variety of resources for data of structural AFPs collection, the Research Collaboratory for Structural Bioinformatics Protein Data Bank (RCSB PDB) has been invested in tools and resources of antifreeze proteins (25). In this research, there are five structural antifreeze proteins which was clarified based on four main strategies. Firstly, the research focus on diversity mechanisms of antifreeze proteins base on discrete structure from different species that involve plant, bacteria, insect and fish were collected in PDB-101. 1HG7 is a PDB entry which belongs to type III antifreeze protein of *Macrozoarces americanus* which eelpout ocean is common name, corresponding to the protein sequence code P19614 and the 1HG7 PDB high-resolution X-ray diffraction refined at $1.15\dot{A}$ resolution from individual anisotropic temperature factors parameter. In order, 3ULT, 3P4G and 1N4I entries of antifreeze protein structures were collected from Prennial ryegrass (*Lolium perenne*) with $1.4\dot{A}$ in resolution of plant, with $1.7\dot{A}$ in resolution of Antarctic bacterium (*Marinomonas*), spruce budworm (*Choristoneura fumiferana*), respectively. All of PDB entries were collected for molecular dynamic simulation using X-ray diffraction for structural constructing.

Martini coarse-grained protein force field, specifically, martinize version 2.3, February 13 2013 and martini v2.1_aminoacids.itp, containing 21 amino acids coarse grained force field, were applied to convert (all-atoms) atomistic antifreeze proteins structure existing as PDB format files into one Coarse Grained (CG) beads, with my

CG protein models, each amino acid is modeled by one or two beads according to their sizes in which can be classified into two broad categories: backbone bead and side-chain bead. The side chain and backbone beads can be denoted as SCi (i = ARG, GLN, GLU, HIS, ILE, LYS, MET, PHE, TRP, TYR) and BBi (i = ALA, ASN, ASP, CYS, GLY, LEU, PRO, SER, THR, VAL), respectively. Some small side-chains of amino acids are avoided due to only existing of one backbone bead while others were modeled by one uniform backbone bead and one distinct side-chain bead each residue has one backbone bead and zero or more side-chain beads depending on the amino acid type.

In the next steps, the CG-AFPs were introduced into the box would be solvate with full coarse grained water molecules which represented as polar type in the MARTINI force field using equilibrated water at 1 atm and 300k and time step of 40 femtosecond. Lennard Jones and Coulomb interactions were calculated very step for atoms within 1.2nm according t of neighbor list which updated every 10 steps. Then, all simulations were performed a short energy minimization before starting production run with for solvated box files using a same standard input options for martini 2.0/2.1 which describe the parameter for running the simulation, including distance step equals 1 femtosecond for 10000000 steps, electrostatics and Van der waals were set at 1.2Å, temperature coupling at 271K using Berend thermostat in equation 1 (spc water model) which approximately about -2^0C based on Berendsen thermostat, and pressure at 1 atm during 10 ns. Besides, atomistic simulation were running using TIP5P water model to provide more detailed information.

$$\frac{dT}{dt} = \frac{T0-T}{\tau} \tag{1}$$

The Berendsen thermostat is an algorithm to re-scale the velocities of particles in molecular dynamics simulations to control the simulation temperature (T) in which the temperature of the system (T) is corrected such that the deviation exponentially decays with some time constant τ.

Further in data analysis, the root means square deviation (RMSD) was used to measure stable in structure of four types of antifreeze proteins follow RMSD equation which was calculated by least-square fitting the structure to the reference structure ($t_2 = 0$) and subsequently calculating the RMSD in equation 2:

$$RMSD(t_1, t_2) = \left[\frac{1}{M}\sum_{i=1}^{N} m_i \|\mathbf{r}_i(t_1) - \mathbf{r}_i(t_2)\|^2\right]^{\frac{1}{2}} \tag{2}$$

Where $M=\sum_{i=1}^{N} m_i$ and $r_i(t)$ was the position of atom i at time t. In this thesis, carbon alpha was used as computing units for RMSD. Additionally, the radius of gyration (R_g) was applied to measure the size and compactness of AFPs base on equation 3:

$$R_g = \frac{1}{N}\sum_{k=1}^{N}(r_k - r_{mean})^2 \tag{3}$$

With N is number of coarse-graining atoms and r_k is the root mean square standard deviation of k atom(s). To ensure the state of coarse-graining water beads in box existing as an icy, the radial distribution function (RDF) or pair correlation function $g_{AB}(r)$ Between the particles of type A and B is defined by the following equation 4:

$$g_{AB}(r) = \frac{\langle \rho_B(r) \rangle}{\langle \rho_B \rangle local} = \frac{1}{\langle \rho_B \rangle local} \frac{1}{N_A} \sum_{i \in A}^{N_A} \sum_{i \in B}^{N_B} \frac{\delta(r_{ij} - r)}{4\pi r^2} \quad (4)$$

$$\text{Or} \quad g(r) = n(r)/(\rho 4\pi r^2 \delta r)$$

With $\langle \rho_B(r) \rangle$ the particle density of type B at a distance r around particles A, and $\langle \rho_B \rangle local$ the particle density of type B averaged over all spheres around A with radius r_{max} which was half of the box length. The averaging was also performed in time. In alternative $g(r)$ formula, $n(r)$ is the number of atoms in a shell δr is shell thickness at r shell radius and ρ is the system density, (Fig. 1).

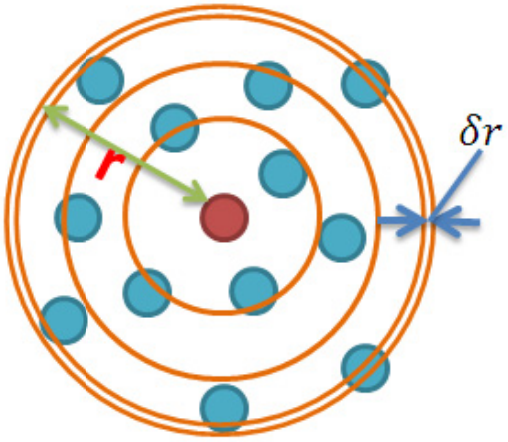

Fig. 1. Radial distribution function of the blue atoms around the red atom with r shell radius and δr shell thickness

2.2 Coarse-Grained Force Field

With the details mentioned antifreeze protein Coarse-Grained models, all internal interactions of a protein can be simplified under the CG force field which can be formulated as equation 5:

$$U = U_{bond} + U_{angle} + U_{torsion} + U_{vdw} + U_{elec} \quad (5)$$

Where U_{bond}, U_{angle} and $U_{torsion}$ are the stretching potential energy of a virtual bond, the potential of a virtual angle bending and the potential function of a dihedral angle are about a rotating bond, respectively, which describe the bonded interactions between CG beads. U_{vdw} and U_{elec} describe the non-bonded interactions, which are the energy of van der Waals interactions and electrostatic interactions respectively. The

virtual stretching interaction between two bonded cg beads can be described as a harmonic potential (equation 6):

$$U_{bond} = \sum \frac{1}{2} K_{bond}(1 - L_{bond})^2 \tag{6}$$

In which K_{bond} and L_{bond} are the force constant and the equilibrium stretching length of a bond, respectively, which would be determined by fitting the energy distribution of the virtual bond. Due to the coarse-graining, U_{angle} and $U_{torsion}$ curves become more complex and irregular when compared with those in AA force field, and they are described with Gaussian distribution function:

$$U_{angle/torsion} = \sum_{i=1}^{N} a_i \exp\left[-\left(\frac{x - b_i}{c_i}\right)^2\right] \tag{7}$$

Where N, a_i, b_i, c_i are Gaussian parameters need to be determined in the parameterization process.

One of important equations of constructing CG-MD force field is the non-bonded potential. As in a classic AA force field, the non-bonded interaction can be divided into two categories, involving van der Waals interaction (U_{vdw}) and electrostatic interaction (U_{elec}). They can be formulated as sums of pairwise potential energy:

$$\begin{aligned} U_{vdw} &= \textstyle\sum_{i<j} 4\varepsilon_{ij}\left(\frac{c_{ij}^{12}}{r_{ij}} - \frac{c_{ij}^{6}}{r_{ij}^{6}}\right) \\ U_{elec} &= \sum_{i<j} \frac{Q_i Q_j}{4\pi\varepsilon_0 \varepsilon_r r_{ij}} \end{aligned} \tag{8}$$

Where c_{ij} is the van der Waals interaction parameter, r_{ij} is the distance between CG beads i and j, and Q_i and Q_j are the charges of i and j. The strength of the van der Waals interaction is determined by the value of well depth ε_{ij} which depends on the types of the interacting CG beads and can be determined in the force field parameterization process for all the 20 types of CG beads. In the coarse-graining, a group of atoms is treated as a single bead, and the relative positions of these atoms are fixed, but in reality, their relative positions vary in all the time.

3 Result and Discussion

3.1 Stability of Antifreeze Proteins

As the very first step to evaluate result's simulation that was relevant was based on for further data analysis, the popular root means square deviation, which used to evaluate structural similarity follow equation 2 by least-square fitting the structure to the reference structure ($t_2 = 0$) and subsequently calculating the RMSD of different types

of antifreeze proteins were utilized for comparing positions of coarse grained atoms and atomistic simulation of a set of initial positions, Carbon-alpha with Carbon-alpha beads of trajectories simulated files.

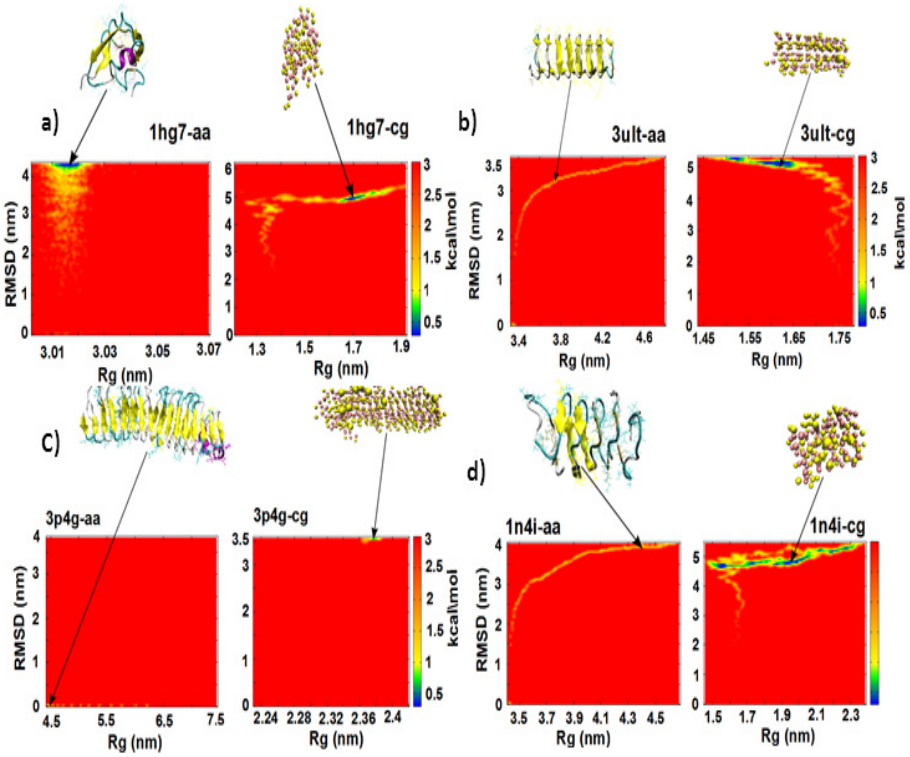

Fig. 2. The root means square deviation, radius of gyration (R_g) and free energy for protein folding. These figure shows the root means square deviation (RMSD) of back-bone carbon of (a) ocean pout (*M. Americanus*) type III antifreeze protein (1HG7) was equilibrium around about 4.5 nm in AA-MD and 5nm in CG-MD that results was higher than (b) antifreeze protein of perennial ryegrass (*L. perenne*, 3ULT) 3.2 nm and 5nm. Two remained antifreeze proteins of (c) marine bacteria (*Marinomonas primoryensis*, 3P4G) and (d) antifreeze protein of spruce budworm (*Choristoneura fumiferana,* 1N4I) which have high similarity in structure, were stable at 0.1nm and 3.5nm, at 4nm and 5nm for equilibrium, respectively.

In RMSD results, the CG-MD gave high 1 nm in average by reducing the number of atoms in AFPs' structure while the AA-MD used to keep the original structures due to the increasing number of atoms (N) of radius of gyration (R_g) equation (Eq. 3), it was larger about double times in all of case between AA-MD and CG-MD, at 4.5nm for AA-MD and 2.3nm for CG-MD in 1N4I; 4.5nm and 2.38nm in 3P4G; 3nm and 1.7nm in 1HG7 and 3.2nm and 1.65nm in 3ULT, respectively. In contrast, the folding energy were not dramatically different in AA/CG simulation arrange from 0.5 to 1 kcal/mol.

3.2 Ice Formation

All of water molecules existed as beads in Coarse Grained simulation, which cannot be evaluated ice formation based on using g_energy analysis tools in Gromacs package 4.6 to plot the bulk density of the system as a function of time of NPT simulations from bond details of atoms to atoms. By that reason, radial distribution function, called g(r), was calculated to ensure all of water beads in system that were ice. The non-periodic between ρ system density and $n(r)$ number of atoms found on shell caused to variety values of $g(r)$ in which two water beads of 1HG7 system was about 5 $\dot{A}$, following that value was 3ULT, 3P4G and 1N4I (Fig. 8). All of water beads in four systems got a long range structural ordering that gave out the solid state of water beads which were ice clusters.

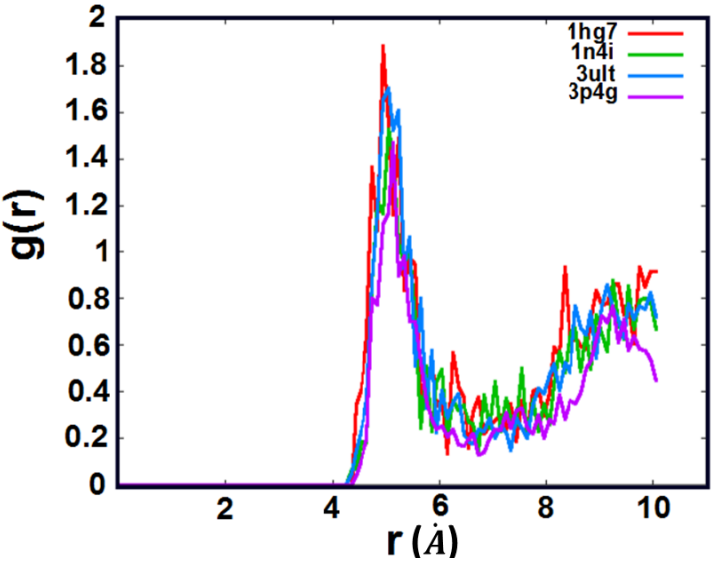

Fig. 3. Result of radial distribution function of coarse-graining water beads in four systems

Firstly, at short separations about $r < 4.3\dot{A}$ the radial distribution function (Fig. 8) was zero that indicated the effective width of the CG water beads, since they cannot approach any more closely. Secondly, the peak appear, which indicated that the CG water beads distance between two coarse graining water beads pack around each other in shell radius that was 5 $\dot{A}$ of distance (r) for all of four antifreeze proteins. The long ranges of the occurrence of peaks were a high degree of ordering while at -2^0C they were very sharp which were in crystalline where atoms are strongly confined in their positions. At very long range, CG water beads had dramatically fluctuated because the radial distribution function describes the average density in this range. In contrast, AA-MD, the short separation about $r < 1.7\dot{A}$ for all of antifreeze proteins that

showed reduced thermal dynamics of TIP5P water molecules in low temperature because the TIP5P freezing point is lower than water freezing point in ambient condition. So, the water molecules in atomistic level still remained liquid phase (Fig. 9).

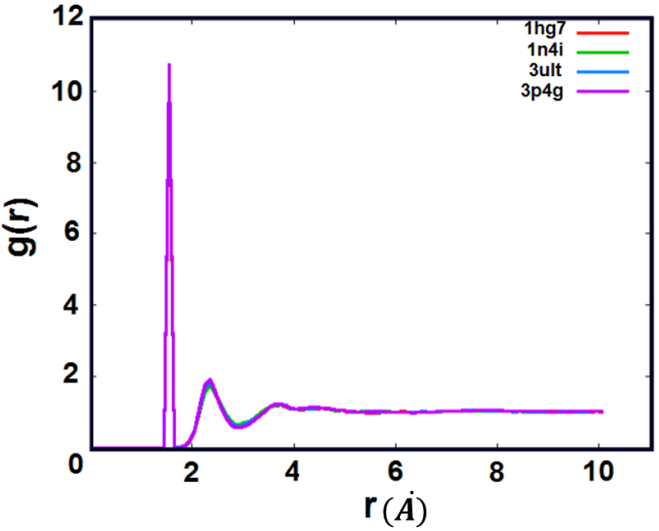

Fig. 4. Result of radial distribution function of TIP5P water molecules in four systems

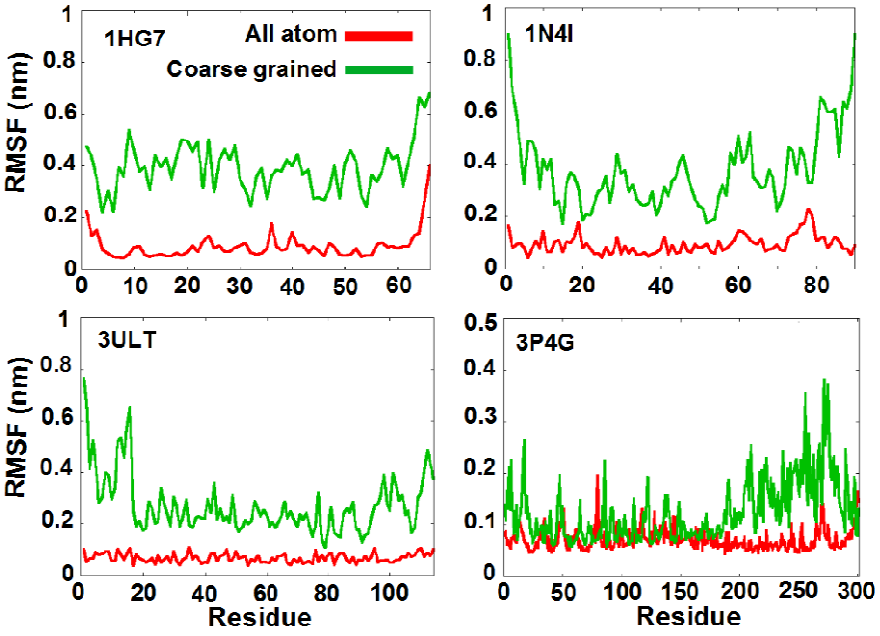

Fig. 5. Root mean square fluctuation of CG/AA models of 1HG7, 1N4I, 3ULT and 3P4G

3.3 Residues Fluctuation of AFPs

By comparing between CG-models and AA-models, the root mean square fluctuation (RMSF) of CG models frequently vibrate in a wide range from 0.2nm to 0.5nm in 1HG7; 0.2nm to 0.9nm in 1N4I; 0.2nm to 0.8nm in 3ULT and 0.15nm to 0.4 in 3P4G against a little change of atomistic simulation in Fig. 10. The main mobility in 1HG7 belong to freely movement of tail from residue 60 to 66 (MET, VAL, LYS, TYR, ALA and ALA) and was the same in a long tail of 3P4G from residue 270 to 300 (TYR, ASN, ASN, SER, SER, ASP, LEU, ARG, ASN, ARG, VAL, ALA, ASN, PHE, GLU, HIS, ILE, ARG, VAL, SER, ASP, GLY, VAL, VAL, LYS, GLY, SER, SER, PRO, ALA, ASP, PHE) while three remained structure had differ to coupling results between CG and AA models occurred in two tail of 3ULT and 1N4I.

4 Conclusion and Recommendation

By studying antifreeze protein from four different types of antifreeze proteins in both all atoms and coarse grained models, the results are first drawing about fluctuation residues by RMSD that is ALA and ALA residues at position 65 and 66 belong to longest tail of 1HG7, the long tail including more than 30 residues in protein sequence of 3ULT which do not play crucial role in ice binding side that regularly arrange on beta-helix motif. Specifically, 1N4I and 3ULT have been stable in binding site which kept beta sheet structure during molecular dynamics simulation running. Although, the mismatch between CG and AA was not relevant for 1N4I and 3ULT came from reducing many potential in details.

5

This study recommends to build a new hybrid simulation between all-atoms and coarse grained molecular simulation will be applied to certain residues for optimized computing complex by reducing the number of atoms in 1HG7 and 3ULT systems that will at least hundred times faster than all-atoms molecular dynamic. Besides, the coarse grained simulation needs to be studied further for 3P4G and 1N4I systems by fluctuated residues which may be affected to ice bind sites. Additionally, molecular simulation cannot stand alone without the experiment up to date but it is utilized to support narrow understood of experiment, as small as picoseconds in interactions between waters and antifreeze proteins.

Acknowledgements. The work was funded by the Department of the Navy, Office of Naval Research under grant number N62909-12-1-7121. Computing resources and support by the Institute of Computational Science and Technology at the Ho Chi Minh City is gracefully acknowledged.

References

1. Atıcı, O., Nalbantoglu, B.: Antifreeze proteins in higher plants. Phytochemistry 64, 1187–1196 (2003)
2. Griffith, M., Yaish, M.W.F.: Antifreeze proteins in overwintering plants: a tale of two activities. Trends Plant Sci. 9, 399–405 (2004)
3. DeVries, A.L., Komatsu, S.K., Feeney, R.E.: Chemical and physical proper-ties of freezing-point depressing glycoproteins from antarctic fishes. J. Biol. Chem. 245, 2901–2908 (1970)
4. Davies, P.L., Hew, C.L., Fletcher, G.L.: Fish antifreeze proteins: physiology and evolutionary biology. Can. J. Zool. 66, 2611–2617 (1980)
5. Marshall, C.B., Fletcher, G.L., Davies, P.L.: Hyperactive antifreeze protein in a fish. Nature 429, 153 (2004)
6. Hew, C.L., Kao, M.H., So, Y.-P., Lim, K.-P.: Presence of cystine-containing antifreeze proteins in the spruce budworm, Choristoneura fumirana. Can. J. Zool. 61, 2324–2328 (1983)
7. Schneppenheim, R., Theede, H.: Isolation and characterization of freezing-point depressing peptides from larvae of Tenebrio molitor. Comp. Biochem. Phys. B. Biochem. Mol. Biol. 67, 561–568 (1980)
8. Duman, J.G., Bennett, V., Sformo, T., Hochstrasser, R., Barnes, B.M.: Anti-freeze proteins in alaskan insects and spiders. J. Insect Physiol. 50, 259–266 (2004)
9. Muryoi, N., Sato, M., Kaneko, S., Kawahara, H., Obata, H., Yaish, M.W.F., Yeh, Y., Feeney, R.E.: Antifreeze proteins: structures and mechanisms of function. Chem. Rev. 96, 601–618 (1996)
10. Yeh, Y., Feeney, R.E.: Antifreeze proteins: structures and mechanisms of function. Chem. Rev. 96, 601–618 (1996)
11. Ewart, K.V., Lin, Q., Hew, C.L.: Structure, function and evolution of antifreeze protein. Cellular and Molecular Life Sciences (CMLS) 55(2) (1999)
12. Bale, J.S.: Insects and Low Temperatures: From Molecular Biology to Distri-butions and Abundance. Biological Sciences 357(1423), 849–862 (2002)
13. Block, W.: To Freeze or Not to Freeze? Invertebrate Survival of Sub-Zero Temperatures. Functional Ecology 5(2), 284–290 (1991)
14. Duman, J.G., Wu, D.W., Xu, L., Tursman, D., Olsen, T.M.: Adaptations of In-sects to Subzero Temperatures. The Quarterly Review of Biology 66(4) (1991)
15. Dalal, P., Knickelbein, J., Haymet, A.D.J., Sönnichsen, F.D., Madura, J.D.: Hydrogen bond analysis of Type 1 antifreeze protein in water and the ice/water interface. Physical Chemistry Communications 7, 1–5 (2001)
16. Griffith, M., Lumb, C., Wiseman, S.B., Wisniewski, M., Johnson, R.W., Ma-rangoni, A.G.: Antifreeze Proteins Modify the Freezing Process in Planta. Plant Physiology 138(1), 330–340 (2005)
17. Hightower, R., Baden, C., Penzes, E., Lund, P., Dunsmuir, P.: Expression of antifreeze proteins in transgenic plants. Plant Molecular Biology 17, 1013–1021 (1991)
18. Hiroki, N., Yoshinori, F.: Antifreeze proteins: computer simulation studies on the mechanism of ice growth inhibition. Polymer Journal 44, 690–698 (2012)
19. Jia, Z.C., Davies, P.L.: Antifreeze proteins: An unusual receptor-ligand interaction. Trends Biochem. Sci. 27, 101–106 (2002)
20. Chao, H., Hodges, R.S., Kay, C.M., Gauthier, S.Y., Davies, P.L.: A natural variant of type I antifreeze protein with four ice-binding repeats is a particularly potent antifreeze. Protein Sci. 5, 1150–1156 (1996)

21. Leinala, E.K., Davies, P.L., Doucet, D., Tyshenko, M.G., Walker, V.K., Jia, Z.C.: A beta-helical antifreeze protein isoform with increased activity—Structural and functional insights. J. Biol. Chem. 277, 33349–33352 (2002)
22. Marshall, C.B., Daley, M.E., Sykes, B.D., Davies, P.L.: Enhancing the activity of a beta-helical antifreeze protein by the engineered addition of coils. Biochemistry 43, 11637–11646 (2004)
23. Haymet, A.D., Ward, L.G., Harding, M.M., Knight, C.A.: Valine substituted-winter flounder 'antifreeze': preservation of ice growth hysteresis. FEBS Lett. 3(430), 301–306 (1998)
24. Nolan, B.H., Yoshiyuki, N., Sakae, T., Frank, D.S.: Activity of a two-domain antifreeze protein is not dependent on linker sequence. Biophysical Journal 92, 541–546 (2007)
25. Rose, P.W., Bi, C., Bluhm, W.F., Christie, C.H., Dimitropoulos, D., Dutta, S., Bourne, P.E.: The RCSB Protein Data Bank: new resources for research and education. Nucleic Acids Res. 41(Database issue), D475–D482 (2013)
26. Gilbert, J.A., Christine, P.J., Dodd, E.R., Layborn-Parry, J.: Demonstration of Antifreeze Protein Activity in Antarctic Lake Bacteria. Microbiology 150, 171–180 (2004)